ISSN 1070-4280, Russian Journal of Organic Chemistry, 2023, Vol. 59, No. 4, pp. 663–673. © Pleiades Publishing, Ltd., 2023.

A Simple, Green, and Efficient One-Pot Synthesis of Dihydropyrano[3,2-*c*]chromene Derivatives Using $MgMnO_3$@ZrO_2@CoO as a Core–Shell Nanocrystalline Catalyst

Y. R. Shelke[a], V. D. Bobade[b], D. R. Tope[b], J. A. Agashe[b], and A. V. Borhade[b,*]

[a] *Department of Chemistry, K. K. Wagh Arts, Commerce and Science College, Pimpalgaon (B), Affiliated to Savitribai Phule Pune University, Nashik, Maharashtra, 422209, India*

[b] *Department of Chemistry, Research Centre, H.P.T Arts and R.Y.K. Science College, Nashik, Maharashtra, 422005, India*

**e-mail: ashokborhade2007@gmail.com*

Received April 17, 2022; revised July 27, 2022; accepted August 14, 2022

Abstract—A rapid, clean, and highly efficient method for the synthesis of dihydropyrano[3,2-*c*]chromene derivatives by one-pot three-component condensation of aromatic aldehydes, malononitrile, and 4-hydroxycoumarin using novel $MgMnO_3$@ZrO_2@CoO core–shell nanocrystalline catalyst is described. The catalyst has been synthesized by hydrothermal method and characterized by XRD, SEM, TEM, and BET surface area analyses. The average particle size of the nanocrystalline catalyst was estimated by TEM scans at 50–60 nm. The BET surface area of $MgMnO_3$@ZrO_2@CoO was found to be 31.61 m^2/g, indicating that it has good catalytic properties. The catalyst can be reused for five successive runs without significant loss in activity. The advantages of the proposed method and catalyst are clean reaction, short reaction time, good yield, easy purification, and reusability and financial availability of the catalyst.

Keywords: dihydropyrano[3,2-*c*]chromene derivatives, $MgZrO_3$@Fe_2O_3@ZnO catalyst, reusable catalyst

DOI: 10.1134/S1070428023040152

INTRODUCTION

Multicomponent reaction (MCRs) are a powerful tool for the synthesis of wide range organic molecules by creating carbon–carbon and carbon–heteroatom bonds in one pot [1–3]. These reactions have various advantages such as simple procedures, high bonding efficiency, low costs, and time and energy saving [4]. MCRs provide greater atom economy and selectivity than traditional multistep syntheses, as well as quick access to molecular complexity and diversity while producing fewer by-products. As a result, MCRs are becoming more vital in modern organic chemistry and are being designed to efficiently produce medicinally relevant scaffolds [5–7].

Heterogeneous catalysts are of great scientific and commercial interest due to their stability, selectivity, and high activity. There is little doubt that the catalysis community keeps a close eye on the progress in nanotechnology [8–10]. In recent years, core–shell nanoparticles have received a lot of interest because of their nanoscale dimensions and unique properties. Core–shell nanoparticles are more stable than pure magnetic particles because the shell protects the magnetic core nanoparticles from environmental degradation and also prevents agglomeration [11–14]. The production of nanoparticles of diverse materials (metallic, semiconductor, and dielectrics) has generated much interest due to their applications in catalysis, medicine, electronics, and other domains. Materials scientists are always exploring innovative ways to change the size and shape of nanoparticles in order to suit the requirements of their applications [15].

Pyrano[3,2-*c*]chromenes constitute an important family of heterocycles with a variety of biological activities, including antispasmodic, diuretic, anticoagulant, anticancer, and anti-anaphylactic action [16, 17]. Furthermore, they have been used to treat Alzheimer's disease, vascular dementia, Huntington's disease, amyotrophic lateral sclerosis, AIDS-related dementia,

and Down's syndrome, as well as schizophrenia and myoclonic seizures [18]. Aminochromene derivatives also have a wide range of biological effects such as antihypertensive and anti-ischemic properties [19–21].

The three-component condensation of 4-hydroxycoumrin, aldehydes, and malononitrile for the synthesis of dihydropyrano[3,2-*c*]chromene derivatives has been carried out under various conditions by using different catalysts such as Fe_3O_4@GO-naphthalene-SO_3H nanocatalyst [22], Fe_3O_4@SiO_2-polyacrylic acid nanocatalyst [23], MNPs@Cu nanocatalyst [24], ionic liquids [25], DABCO [26], $Mg(ClO_4)_2$ [27], $AcONH_4$ [28], DBU [29], diammonium hydrogen phosphate (DAHP) [30], Na_2HPO_4 [31], K_2CO_3 [32], (*S*)-proline [33], tetrabutylammonium bromide (TBAB) [34], 3-hydroxypropanaminium acetate (HPAA) [35], [bmim]Br [36], and potassium phthalimide-*N*-oxyl [37]. These catalysts have some drawbacks related to high costs, high reaction temperatures, low yields, the use of hazardous solvents, and the need for specialized equipment, which produced negative results.

In view of the above results, herein we used $MgMnO_3$@ZrO_2@CoO core–shell catalyst for the synthesis of dihydropyrano[3,2-*c*]chromenes that have a wide range of pharmacological, biological, and therapeutic effects using a simple and ecofriendly technique.

RESULTS AND DISCUSSION

The $MgMnO_3$@ZrO_2@CoO core–shell catalyst was prepared as shown in Scheme 1. Initially, $MgMnO_3$ nanoparticles were synthesized by the hydrothermal process from equivalent amounts of magnesium chloride ($MgCl_2$) and manganese chloride ($MnCl_4$) in double distilled water in the presence of polyethylene glycol, followed by treatment with aqueous sodium hydroxide. Next, $MgMnO_3$@ZrO_2 core–shell nanoparticles were obtained by dissolving $MgMnO_3$ and ZrO_2 [38] (1:2) and an appropriate quantity of polyethylene glycol in double distilled water. Finally, $MgMnO_3$@ZrO_2 was treated with an equimolar amount of cobalt(II) oxide [38] in 2 M NaOH in the presence of polyethylene glycol. The resulting nanocatalyst was calcined for 6 h at 700°C.

XRD analysis. The $MgMnO_3$@ZrO_2@CoO core–shell catalyst was characterized by XRD, SEM, TEM, EDAX, and BET surface area analyses. Figure 1 shows the XRD patterns of $MgMnO_3$, $MgMnO_3$@ZrO_2, and $MgMnO_3$@ZrO_2@CoO. All diffraction peaks in the XRD pattern of $MgMnO_3$ (Fig. 1a) were indexed to a defect cubic spinel-type structure (JCPDS, 28-0625) with well-ordered *hkl* planes. The diffraction peaks (111), (220), (311), (222), (400), (422), (511), (440), (533), and (622) were seen at different diffraction angles of 18.07°, 30.97°, 36.08°, 36.61°, 44.34°, 53.88°, 56.17°, 64.50°, 74.18°, and 76.52°. The presence of ZrO_2 in $MgMnO_3$@ZrO_2 was confirmed by its XRD pattern (Fig. 1b) which displayed broad peaks at 28.29°, 30.37°, and 31.54°. According to the JCPDS 79-1771 card, the peak centered at 30.37° (101) is typical of the tetragonal crystalline phase, whereas those at 28.29° (111) and 31.54° (111) are representative of the monoclinic phase (JCPDS 37-1484). These findings point to a combination of tetragonal and monoclinic crystalline phases that are seen in ZrO_2 materials [39, 40]. Figure 1c shows the presence of ZrO_2 and CoO phases in the $MgMnO_3$@ZrO_2@CoO core–shell nanoparticle clusters suggesting that CoO was coated on the ZrO_2 nanoparticles. The major peaks were found at 36.92°, 44.78°, and 65.32°, corresponding to the lattice scattering planes (111), (200) and (220) for CoO crystal. Also, well-defined peaks assigned to the face-centered cubic structures were observed, which matched with the JCPDS card 071-1178 for cobalt oxide [41, 42].

Scanning electron microscopy (SEM) analysis. The morphology of the core–shell nanoparticles was

Scheme 1.

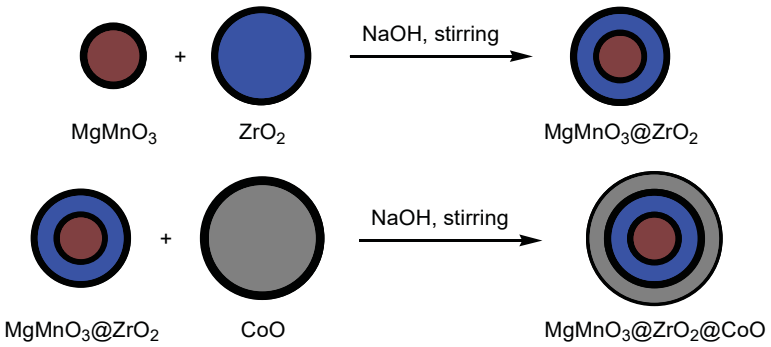

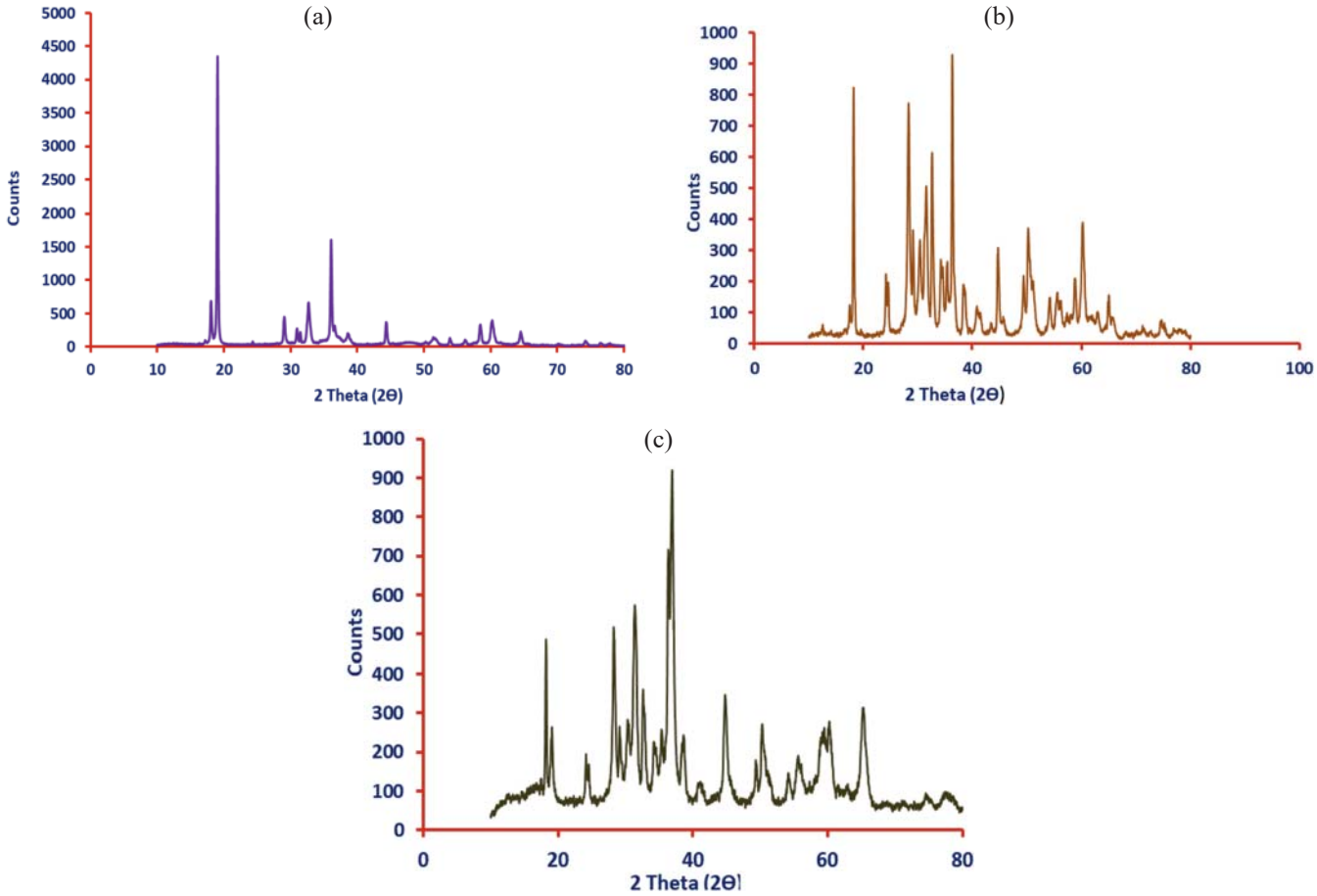

Fig. 1. XRD patterns of (a) $MgMnO_3$, (b) $MgMnO_3@ZrO_2$, and (c) $MgMnO_3@ZrO_2@CoO$.

examined by field-emission scanning electron microscopy (FE-SEM). Figure 2a shows the FE-SEM micrograph of pure magnesium magnate particles generated by the sol–gel process. As verified by the XRD data, cubic and octahedral morphologies can be seen with the crystal habit of spinel minerals. The $MgMnO_3@ZrO_2$ crystals are larger than $MgMnO_3$ (Fig. 2b). The crystals are cubic and rectangular with sharp edges. The crystals of $MgMnO_3@ZrO_2@CoO$ core–shell nanoparticles are smaller and are cubic and rectangular in shape (Fig. 2c).

Energy dispersive X-ray spectroscopy (EDAX) analysis. The elemental composition of $MgMnO_3$ coated with ZrO_2 and CoO was investigated by using energy-dispersive X-ray spectroscopy. Figure 2a revealed the prominent peaks for magnesium at 1.2 keV and manganese at 0.7 and 5.8 keV in the EDAX spectrum, whereas zirconium was found at 2.1 keV in $MgMnO_3$ coated with ZrO_2, as displayed in Fig. 2b on the same scale as for $MgMnO_3$. The EDAX spectrum of $MgMnO_3@ZrO_2$ covered with cobalt oxide confirmed the presence of the latter which gave peaks at 0.5, 7.1, and 7.8 keV due to Co (Fig. 2c). Thus, the presence of Mg, Mn, O, Zr, and Co with appropriate proportions in the prepared core–shell nanoparticles has been demonstrated.

Transmission electron microscopy (TEM) analysis. For further investigation of shape and size, TEM analysis was performed for $MgMnO_3$, $MgMnO_3@ZrO_2$, and $MgMnO_3@ZrO_2@CoO$ (Fig. 3). It is known that TEM analysis gives accurate information about the morphology of nanostructures. The TEM analysis of $MgMnO_3$ nanoparticles revealed their cubic shape and a crystal size of 40–50 nm (Fig. 3a). Figure 3b shows a typical TEM image of $MgMnO_3@ZrO_2$ core–shell nanoparticles prepared from zirconium oxide precursor with hexagonal structure which formed layers on the surface of the $MgMnO_3$ core after thermal degradation. The particle size is 55–60 nm. Figure 3c shows the TEM image of a double coated $MgMnO_3$ sample confirming the presence of two kinds of coating layers on the $MgMnO_3$ core. The ZrO_2 shell surrounds the $MgMnO_3$ core as a primary coating layer, while CoO covers the ZrO_2 shell as a secondary coating layer. It is

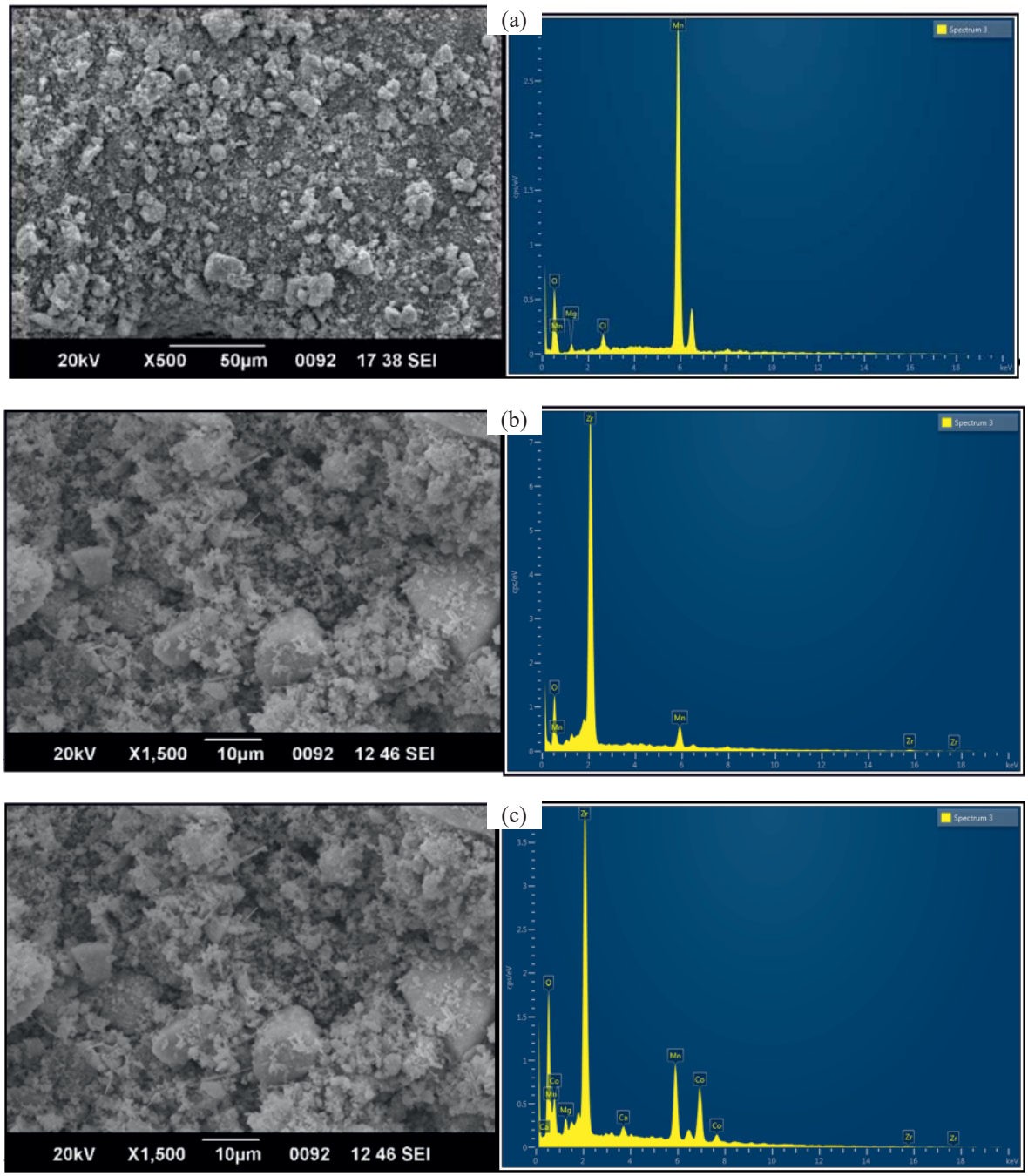

Fig. 2. SEM micrographs and EDAX spectra of a) $MgMnO_3$,, b) $MgMnO_3$@ZrO_2, and (c) $MgMnO_3$@ZrO_2@CoO.

seen that CoO forms a full solid coating layer on ZrO_2. The particle size of $MgMnO_3$@ZrO_2@CoO is 30–35 nm.

Brunauer–Emmett–Teller (BET) analysis. Measurements of the specific surface area, pore size, and pore volume of core–shell nanomaterials are important since their surface characteristics are responsible for their interfacial behavior when they are used as catalysts. The surface area (S_{BET}), pore size, and pore volume of the synthesized catalyst were determined according to the Brunauer–Emmett–Teller (BET) method by measuring nitrogen adsorption. The N_2 adsorption–desorption isotherms for $MgMnO_3$, $MgMnO_3$@ZrO_2, and $MgMnO_3$@ZrO_2@CoO are shown in Fig. 4. According to the BDDT classification, the adsorption curves in Fig. 4a–4c correspond to type III. The surface areas (S_{BET}), pore diameters (d_p), and pore volumes (V_p) are given in Table 1.

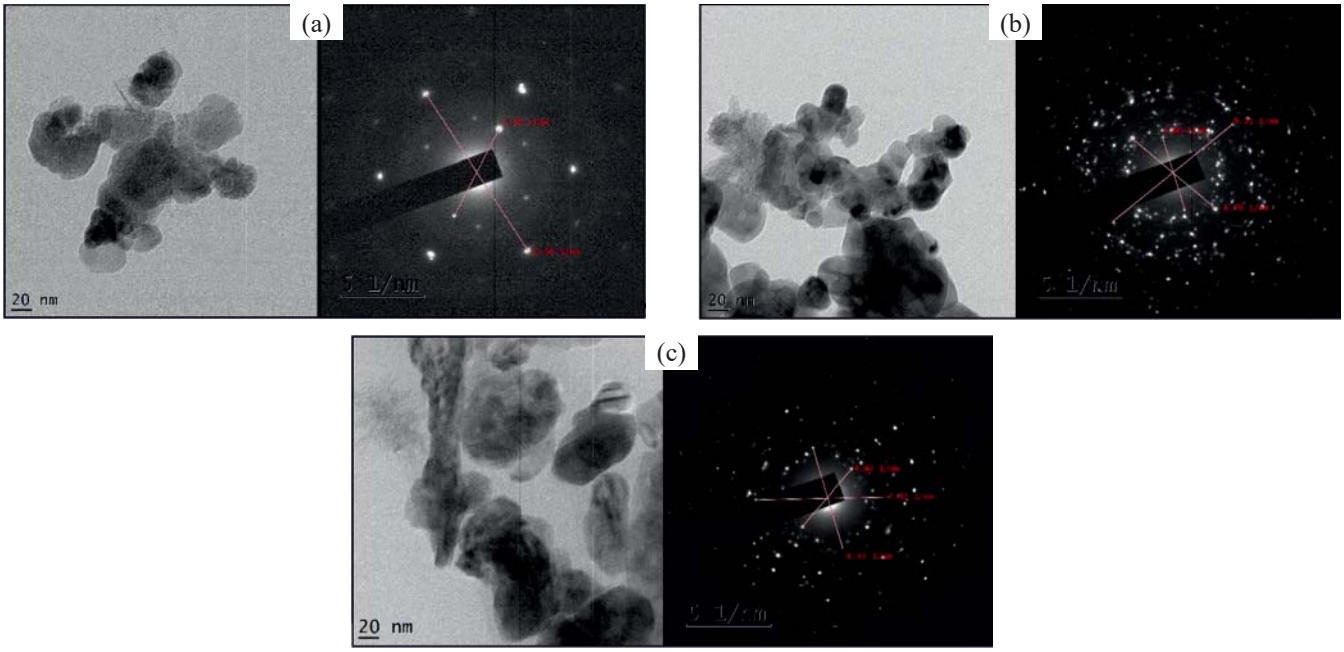

Fig. 3. TEM images and SAED patterns of (a) $MgMnO_3$, (b) $MgMnO_3@ZrO_2$, and (c) $MgMnO_3@ZrO_2@CoO$.

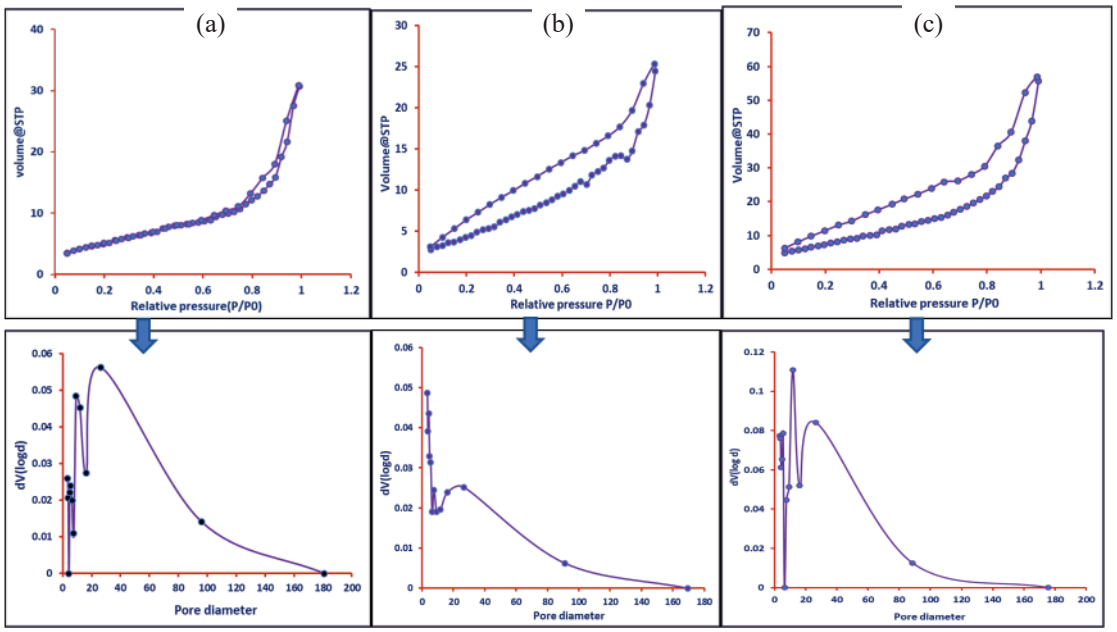

Fig. 4. BET Surface area analysis of (a) $MgMnO_3$, (b) $MgMnO_3@ZrO_2$, and (c) $MgMnO_3@ZrO_2@CoO$ nanoparticles.

The prepared $MgMnO_3@ZrO_2@CoO$ core–shell nanocatalyst was used in the condensation of 4-hydroxycoumarin (**1**), malononitrile (**2**), and substituted benzaldehydes **3a**–**3j** to obtain dihydropyrano[3,2-*c*]-chromene derivatives **4a**–**4j** (Scheme 2). To optimize the conditions, the condensation of 4-nitrobenzaldehyde (**3b**, 1 mmol), 4-hydroxycoumarin (**1**, 1 mmol), and malononitrile (**2**, 1.1 mmol) was selected as a model reaction. First, the catalytic efficiency of $MgMnO_3$, $MgMnO_3@ZrO_2$, and $MgMnO_3@ZrO_2@CoO$ nanoparticles in the model reaction was studied. The results showed that $MgMnO_3@ZrO_2@CoO$ efficiently catalyzed the reaction and that 0.3 g of the catalyst produced the best yield (Table 2). Neither decrease or increase of the amount of $MgMnO_3@$-$ZrO_2@CoO$ affected the yield or reaction time.

Table 3 summarizes the results of studying the effects of solvent and temperature on the reaction. The

Scheme 2.

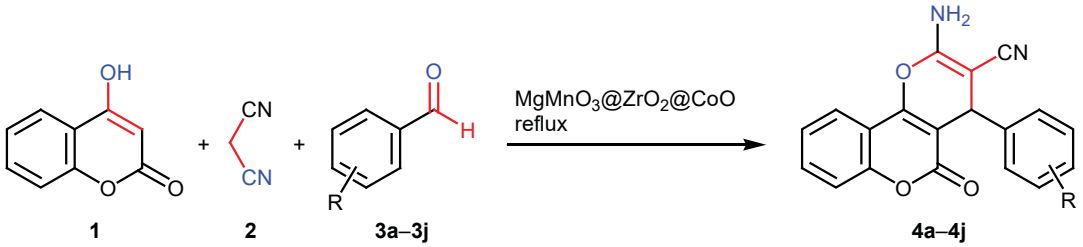

For R, see Table 4.

condensation of 4-nitrobenzaldehyde, 4-hydroxycoumarin, and malononitrile was carried out in chloroform, acetonitrile, *N*,*N*-dimethylformamide, methylene chloride, ethanol, methanol, and water. When the reaction was carried out under solvent-free conditions at room temperature, no target product was formed even after 20 min, but the yield of **4b** was 68% under reflux condition (Table 3; entry nos. 1, 2). When chloroform was used as a solvent, the yield was extremely low at the reflux temperature (Table 3, entry no. 3), the reaction time being the same. The use of a more polar solvent such as acetonitrile under reflux did not improve the yield to a significant extent (Table 3, entry no. 4). Likewise, no significant results were obtained

Table 1. BET surface area, pore diameter (Dp), and pore volume (Vp) of core shell nanoparticles

Catalyst	BET surface area S_{BET}, m^2/g	Pore diameter d_p, nm	Pore volume V_p, cm^3/g
$MgMnO_3$	18.43	10.32	0.004573
$MgMnO_3@ZrO_2$	15.25	3.385	0.03157
$MgMnO_3@ZrO_2@CoO$	31.61	3.386	0.07753

Table 2. Effect of catalyst on reaction time and yield of **4b** in 20 min

Entry. no.	Catalyst	Amount of catalyst, g	Yield of **4b**, %
1	$MgMnO_3$	0.3	57
2	$MgMnO_3@ZrO_2$	0.3	68
3	$MgMnO_3@ZrO_2@CoO$	0.1	91
4	$MgMnO_3@ZrO_2@CoO$	0.3	97
5	$MgMnO_3@ZrO_2@CoO$	0.5	92

Table 3. Effect of solvent and temperature on the yield of **4b** in 20 min

Entry no.	Solvent	Temperature	Yield of **4b**, %
1	None	R.T.	No reaction
2	None	Reflux	68
3	Chloroform	Reflux	29
4	Acetonitrile	Reflux	43
5	Dimethyformamide	Reflux	82
6	Dichloromethane	Reflux	67
7	Methanol	Reflux	88
8	Ethanol	Reflux	97
9	Ethanol	R.T.	34

Table 4. Synthesis of substituted dihydropyrano[3,2-*c*]chromene derivatives **4a**–**4j** using $MgMnO_3$@ZrO_2@CoO core–shell catalyst (ethanol, reflux)

Compd. no.	R	Time, min	Yield, %	mp, °C
4a	4-Cl	20	91	267–268 [30]
4b	4-NO_2	20	97	258–260 [30]
4c	4-OMe	35	92	243–245 [30]
4d	3-NO_2	30	89	263–265 [30]
4e	4-Me	40	80	265–268 [30]
4f	4-Br	35	87	246–248 [26]
4g	4-OH	35	86	260–262 [24]
4h	4-F	35	87	260–262 [22]
4i	4-NMe_2	30	91	214–216 [44]
4j	2,4-$(OMe)_2$	45	89	236–238 [43]

using methylene chloride or methanol (Table 3; entry nos. 5, 7). Finally, ethanol was chosen as the best solvent since it provided the maximum yield (Table 3, entry no. 8). Thus, the optimal conditions were 0.3 g of $MgMnO_3$@ZrO_2@CoO catalyst and ethanol as a solvent under reflux; in this case, the reaction was complete in 20 min to afford 97% of **4b**.

The scope of the three-component one-pot condensation was explored using different substituted aromatic aldehydes under the optimized conditions (Table 4). Aromatic aldehydes with both electron-withdrawing and electron-donating substituents gave high yields of the corresponding dihydropyrano[3,2-*c*]-chromene derivatives. The best yield was achieved with 4-nitrobenzaldehyde (**3b**).

Heterogeneous catalysts are advantageous since they can be easily recovered and reused. The recyclability of the catalyst was estimated by carrying out the synthesis of **4b** using recovered $MgMnO_3$@ZrO_2@-CoO. For each cycle, after completion of reaction, product **4b** was isolated and identified. The catalyst could be recovered by simple filtration and reused for five successive runs times without a notable change in the yield and reaction time (Fig. 5). Table 5 compares the $MgMnO_3$@ZrO_2@CoO core–shell catalyst with some previously reported catalysts in terms of reaction time, yield, and conditions.

EXPERIMENTAL

Commercially available magnesium chloride ($MgCl_2$), manganese(IV) chloride ($MnCl_4$), poly-(ethylene glycol), organic compounds, and solvents (anhydrous grade) were used without further purification. Silica gel (80–120 mesh) was used for column chromatography. The melting points were measured in capillary tubes and are uncorrected. The IR spectra were recorded on a Shimadzu IR Affinity FT-IR spectrometer. The ^1H and ^{13}C NMR spectra were recorded on a Bruker spectrometer at 400 and 100 MHz, respectively, using DMSO-d_6 as solvent and tetramethylsilane as internal standard. The mass spectra (electron impact, 70 eV) were obtained on an Agilent Technologies 5975C GC/MS instrument.

The X-ray powder diffraction patterns were obtained by using a Rigaku Ultima IV diffractometer running at 25 kV and 25 mA with Cu K_α radiation (λ 0.154 nm); Bragg's scanning angle 20° to 80°. The elemental compositions and atomic weight proportions of $MgMnO_3$@ZrO_2@CoO were studied using a Bruker

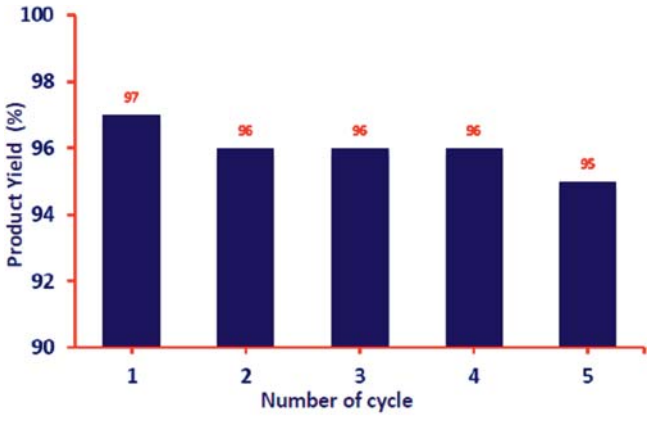

Fig. 5. Reusability of $MgMnO_3$@ZrO_2@CoO catalyst in the synthesis of 2-amino-4-(4-nitrophenyl)-5-oxo-4*H*,5*H*-pyrano[3,2-*c*]chromene-3-carbonitrile (**4b**).

Table 5. Comparison of the catalysts for the synthesis of dihydropyrano[3,2-*c*]chromene derivative **4b**

Entry no.	Catalyst	Time, min	Yield, %	Reference
1	DABCO	30	96	26
2	$Mg(ClO_4)_2$	45	95	27
3	IL-Immobilized $FeNi_3$	15	95	44
4	Trisodium citrate	35	88	45
5	4-Chlorophenylboronic acid	70	89	46
6	$MgMnO_3$@ZrO_2@CoO	20	97	Present work

X-Flash 613 equipment. The surface morphology and characteristics of the material were analyzed with an FEI Nova Nano SEM 450 scanning electron microscope. The crystallinity, shape, and crystal type of $MgMnO_3$ and core-shell nanostructures were studied using a JEOL/JEM 2100 transmission electron microscope (200 kV, LaB6 electron gun, resolution 0.23 and 0.14 nm). The N_2 adsorption–desorption isotherm used to calculate the BET surface area of the catalyst was plotted using a Quantachrome NOVA-1200 Autosorb-1 automated gas sorption system and an Autosorb-1C mercury porosimeter.

Synthesis of $MgMnO_3$ Nanoparticles. A 2 M solution of sodium hydroxide was gently added with vigorous stirring to a mixture of equivalent amounts of magnesium chloride ($MgCl_2$), manganese(IV) chloride ($MnCl_4$), and polyethylene glycol as a surfactant in 100 mL of double distilled water. The mixture was heated at 120°C for 24 h in a Teflon-lined steel autoclave, and the resulting gel was filtered off, repeatedly washed with double distilled water, and dried at 110°C to remove the surfactant.

Synthesis of $MgMnO_3$@ZrO_2 core–shell nanoparticles. A 1 M NaOH solution was added dropwise over a period of 1 h under continuous stirring to a mixture of 1 mol of $MgMnO_3$, 2 mol ZrO_2 [40], and 2 mL of polyethylene glycol in 100 mL of double distilled water. The resulting slurry was autoclaved for 24 h at 120°C, and the precipitate was filtered, washed twice with double distilled water, dried for 5 h at 110°C, and calcined for 6 h at 650°C to eliminate organic impurities.

Synthesis of $MgMnO_3$@ZrO_2@CoO core–shell nanoparticles. A mixture of $MgMnO_3$@ZrO_2 (1 mol), cobalt(II) oxide (1 mol) [40], and 2 mL of polyethylene glycol in 100 mL of 2 M NaOH was gently stirred for 2 h. The mixture was then heated for 24 h at 120°C in a Teflon-lined steel autoclave in an oven. After completion of the reaction, the precipitate was filtered off, washed with deionized water, and dried for 4 h at 120°C. To make a fine powder, the dry product was crushed using a pestle in a mortar, and the resulting powder was calcined for 6 h at 700°C.

General procedure for the synthesis of dihydropyrano[3,2-*c*]chromene derivatives 4a–4j. A mixture of 4-nitrobenzaldehyde (1 mmol), 4-hydroxycoumarin (1 mmol), malononitrile (1.1 mmol), and $MgMnO_3$@ZrO_2@CoO (0.3 g) in 10 mL of ethanol was refluxed with constant stirring for a time indicated in Table 4. When the reaction was complete (TLC), the mixture was cooled to room temperature, transferred into a beaker, and diluted with distilled water. The solid product was filtered off and washed with distilled water and cold ethanol to remove unreacted starting materials and other organic contaminations. The catalyst was separated from the product by filtration using ethanol. The catalyst is insoluble in ethanol, and it could be reused by simple filtration. Compounds **4a**–**4j** were purified by recrystallization from ethanol.

2-Amino-4-(4-chlorophenyl)-5-oxo-4*H*,5*H*-pyrano[3,2-*c*]chromene-3-carbonitrile (4a) was synthesized from 4-chlorobenzaldehyde (**3a**, 1.1 mmol), 4-hydroxycoumarin (1.2 mmol), and malononitrile (1.1 mmol); reaction time 20 min. Yield 0.98 g (91%), dark yellow solid, mp 267–268°C. IR spectrum, ν, cm^{-1}: 778 (C–Cl), 1046 (C–O), 1231 (C–O), 1602 (C=C), 1650 (C=C), 1730 (C=O), 2245 (C≡N), 3122 (=C–H), 3218 and 3310 (NH_2). ^{1}H NMR spectrum, δ, ppm: 4.98 s (1H, 4-H), 7.43 d (2H, H_{arom}, J = 8.2, 7.4 Hz), 7.68 d (2H, H_{arom}, J = 8.2, 7.4 Hz), 9.76 s (2H, NH_2). ^{13}C NMR spectrum, δ_C, ppm: 103.5, 114.4, 115.6, 116.2, 116.3, 118.2, 120.3, 122.3, 122.6, 134.3, 136.4, 138.6, 143.2, 152.5, 158.2, 161.2, 172.3 (C=O). Mass spectrum: *m*/*z* 351.23.

2-Amino-4-(4-nitrophenyl)-5-oxo-4*H*,5*H*-pyrano[3,2-*c*]chromene-3-carbonitrile (4b) was synthesized from 4-nitrobenzaldehyde (**3b**, 1.0 mmol), 4-hydroxycoumarin (1.1 mmol), and malononitrile

(1.1 mmol); reaction time 20 min. Yield 0.97 g (97%), dark yellow solid, mp 258–260°C. IR spectrum, ν, cm^{-1}:1030 (C–O), 1248 (C–O), 1345 (NO_2), 1653 (C=C), 1734 (C=O), 2257 (C≡N), 3217 (=C–H), 3324 (NH_2), 3410 (NH_2). ^1H NMR spectrum, δ, ppm: 5.12 s (1H, 4-H), 7.44 d (2H, *J* = 8.0, 7.2 Hz, H_{arom}), 7.85 d (2H, *J* = 8.0, 7.2 Hz, H_{arom}), 8.47 s (2H, NH_2). ^{13}C NMR spectrum, δ_C, ppm: 102.3, 112.3, 114.5, 114.9, 118.2, 120.1, 122.2, 124.7, 126.6, 130.7, 132.1, 138.6, 148.4, 158.3, 160.2, 164.2, 176.5 (C=O). Mass spectrum: *m*/*z* 363.43.

2-Amino-4-(4-methoxyphenyl)-5-oxo-4*H*,5*H*-pyrano[3,2-*c*]chromene-3-carbonitrile (4c) was synthesized from 4-methoxybenzaldehyde (**3c**, 1.0 mmol), 4-hydroxycoumarin (1.1 mmol), and malononitrile (1.1 mmol); reaction time 35 min. Yield 0.93 g (92%), white solid, mp 243–245°C. IR spectrum, ν, cm^{-1}: 987 (C–C), 1054 (C–C), 1120 (C–C), 1431 (C–C),1656 (C–O), 1728 (C=O), 2235 (C≡N), 3309 (=C–H), 3365 (NH_2). ^1H NMR spectrum, δ, ppm: 2.8 s (3H, OCH_3), 5.09 s (1H, 4-H), 7.59 d (2H, *J* = 8.1, 7.3 Hz, H_{arom}), 7.71 d (2H, *J* = 8.1, 7.3 Hz, H_{arom}), 6.54 s (2H, NH_2). ^{13}C NMR spectrum, δ_C, ppm: 35.7 (OCH_3), 103.2, 114.8, 116.4, 116.5, 119.5, 122.2, 122.5, 126.9, 128.6, 132.3, 132.9, 136.4, 142.2, 154.2, 156.7, 160.4, 172.9 (C=O). Mass spectrum: *m*/*z* 348.97.

2-Amino-4-(3-nitrophenyl)-5-oxo-4*H*,5*H*-pyrano[3,2-*c*]chromene-3-carbonitrile (4d) was synthesized from 3-nitrobenzaldehyde (**3d**, 1.1 mmol), 4-hydroxycoumarin (1.2 mmol), and malononitrile (1.2 mmol); reaction time 30 min. Yield 0.91 g (89%), yellow solid, mp 263–265°C. IR spectrum, ν, cm^{-1}: 984 (C–C),1047 (C–C), 1232 (C–O), 1342 (NO_2),1602 (C–O), 1632 (C–O), 1738 (C=O), 2245 (C≡N), 3123 (=C–H), 3321 (NH_2), 3498 (NH_2). ^1H NMR spectrum, δ, ppm: 4.87 s (1H, 4-H), 7.42 d (2H, *J* = 8.1, 7.2 Hz, H_{arom}), 7.54 d (2H, *J* = 8.1, 7.2 Hz, H_{arom}), 9.98 s (2H, NH_2). ^{13}C NMR spectrum, δ_C, ppm: 104.5, 110.2, 112.4, 116.7, 118.4, 121.5, 122.8, 124.4, 128.9, 132.3, 138.4, 140.8, 142.7, 152.5, 158.6, 162.5, 172.7 (C=O). Mass spectrum: *m*/*z* 363.21.

2-Amino-4-(4-methylphenyl)-5-oxo-4*H*,5*H*-pyrano[3,2-*c*]chromene-3-carbonitrile (4e) was synthesized from 4-methylbenzaldehyde (**3e**, 1.2 mmol), 4-hydroxycoumarin (1.2 mmol), and malononitrile (1.1 mmol); reaction time 40 min. Yield 0.84 g (80%), white solid, mp 265–268°C. IR spectrum, ν, cm^{-1}: 1156 (C–O), 1234 (C–C), 1604 (C–O), 1632 (C–O), 1743 (C=O), 2232 (C≡N), 3294 (=C–H), 3310 (NH_2). ^1H NMR spectrum, δ, ppm:1.8 s (3H, CH_3), 4.97 s (1H, 4-H), 7.38 d (2H, *J* = 8.2, 7.4 Hz, H_{arom}), 7.68 d (2H, *J* = 8.2, 7.4 Hz, H_{arom}), 6.78 s (2H, NH_2). ^{13}C NMR spectrum, δ_C, ppm: 21.2 (CH_3), 103.6, 113.7, 116.8, 116.9, 118.2, 121.2, 122.3, 124.8, 128.9, 131.7, 136.1, 140.6, 142.3, 152.6, 158.6, 162.2, 172.6 (C=O). Mass spectrum: *m*/*z* 332.23.

2-Amino-4-(4-bromophenyl)-5-oxo-4*H*,5*H*-pyrano[3,2-*c*]chromene-3-carbonitrile (4f) was synthesized from 4-bromobenzaldehyde (**3f**, 1.1 mmol), 4-hydroxycoumarin (1.0 mmol), and malononitrile (1.0 mmol) ; reaction time 35 min. Yield 0.89 g (87%), brown solid, mp 246–248°C. IR spectrum, ν, cm^{-1}: 835 (C–Br), 932 (C–C), 1056 (C=C), 1287 (C=C), 1458 (C–N), 1665 (C–O), 1734 (C=O), 2276 (C≡N), 3234 (=C–H), 3376 (NH_2), 3456 (NH_2). ^1H NMR spectrum, δ ppm:4.97 s (1H, 4-H), 7.39 d (2H, *J* = 8.2, 7.2 Hz, H_{arom}), 7.62 d (2H, *J* = 8.0, 7.2 Hz, H_{arom}), 6.98 s (2H, NH_2). ^{13}C NMR spectrum, δ_C, ppm: 104.6, 111.4, 113.6, 116.3, 119.6, 122.1, 122.9, 126.7, 128.4, 130.4, 134.4, 142.1, 146.8, 162.2, 162.8, 166.8, 172.3 (C=O). Mass spectrum: *m*/*z* 396.

2-Amino-4-(4-hydroxyphenyl)-5-oxo-4*H*,5*H*-pyrano[3,2-*c*]chromene-3-carbonitrile (4g) was synthesized from 4-hydroxybenzaldehyde (**3g**, 1.1 mmol), 4-hydroxycoumarin (1.0 mmol), and malononitrile (1.0 mmol); reaction time 35 min. Yield 0.88 g (86%), white solid, mp 260–262°C. IR spectrum, ν, cm^{-1}: 856 (C–H), 1123 (C–C), 1221 (C–C), 1440 (C–O),1634 (C–O), 1734 (C=O), 2234 (C≡N), 3181 (=C–H), 3298 and 3380 (NH_2). ^1H NMR spectrum, δ, ppm: 5.23 s (1H, 4-H), 7.43 d (2H, *J* = 8.1, 7.3 Hz, H_{arom}), 7.72 d (2H, *J* = 8.1, 7.3 Hz, H_{arom}), 6.87 s (2H, NH_2). ^{13}C NMR spectrum, δ_C, ppm: 104.8, 110.1, 110.5, 111.9, 112.2, 118.1, 118.2, 120.7, 122.6, 122.9, 128.1, 128.6, 138.4, 148.3, 150.2, 154.2, 172.5 (C=O). Mass spectrum: *m*/*z* 334.65.

2-Amino-4-(4-fluorophenyl)-5-oxo-4*H*,5*H*-pyrano[3,2-*c*]chromene-3-carbonitrile (4h) was synthesized from 4-fluorobenzaldehyde (**3h**, 1.2 mmol), 4-hydroxycoumarin (1.1mmol), and malononitrile (1.1 mmol); reaction time 35 min. Yield 0.90 g (87%), yellow solid, mp 260–262°C. IR spectrum, ν, cm^{-1}: 775 (C–F), 875 (C–H), 1012 (C–C), 1131 (C–C), 1267 (C–C),1621 (C–O), 1732 (C=O), 2234 (C≡N), 3317 (=C–H), 3424 (NH_2). ^1H NMR spectrum, δ, ppm: 4.95 s (1H, 4-H), 7.32 d (2H, *J* = 8.0, 7.2 Hz, H_{arom}), 7.58 d (2H, *J* = 8.0, 7.2 Hz, H_{arom}), 6.98 s (2H, NH_2). ^{13}C NMR spectrum, δ_C, ppm: 104.6, 108.3, 110.5, 110.9, 111.2, 112.8, 113.2, 114.7, 116.6, 126.7, 128.1, 128.6, 148.9, 149.3, 162.2, 166.8, 172.5 (C=O). Mass spectrum: *m*/*z* 336.78.

2-Amino-4-[4-(dimethylamino)phenyl]-5-oxo-4*H*,5*H*-pyrano[3,2-*c*]chromene-3-carbonitrile (4i) was synthesized from 4-(dimethylamino)benzaldehyde (**3i**, 1.0 mmol), 4-hydroxycoumarin (1.1 mmol), and malononitrile (1.1 mmol); reaction time 30 min. Yield 0.91 g (91%), dark yellow solid, mp 214–216°C. IR spectrum, ν, cm^{-1}: 895 (C–H), 1123 (C–C), 1276 (C–C), 1434 (C–N),1631 (C–O), 1742 (C=O), 2243 (C≡N), 3307 (=C–H), 3376 and 3390 (NH_2). ^{1}H NMR spectrum, δ, ppm: 2.8 s (6H, CH_3), 5.23 s (1H, 4-H), 7.30 d (2H, J = 8.2, 7.3 Hz, H_{arom}), 7.56 d (2H, J = 8.2, 7.3 Hz, H_{arom}), 6.78 s (2H, NH_2). ^{13}C NMR spectrum, δ_C, ppm: 45.3 (CH_3), 103.6, 110.1, 112.1, 112.9, 116.2, 118.8, 120.2, 122.4, 124.6, 128.8, 130.6, 136.2, 142.4, 152.1, 156.2, 160.2, 172.5 (C=O). Mass spectrum: *m*/*z* 362.32.

2-Amino-4-(2,4-dimethoxyphenyl)-5-oxo-4*H*,5*H*-pyrano[3,2-*c*]chromene-3-carbonitrile (4j) was synthesized from 2,4-dimethoxybenzaldehyde (**3j**, 1.1 mmol), 4-hydroxycoumarin (1.2 mmol), and malononitrile (1.1 mmol); reaction time 45 min. Yield 0.90 g (89 %), yellow product, mp 236–238°C. IR spectrum, ν, cm^{-1}: 1134 (C–C), 1435 (C–N), 1542 (C–O), 1632 (C–O), 1747 (C=O), 2242 (C≡N), 3189 (=C–H), 3284 and 3381 (NH_2). ^{1}H NMR spectrum, δ, ppm: 3.24 s (6H, CH_3O), 5.02 s (1H, 4-H), 7.44 d (2H, J = 8.0, 7.2 Hz, H_{arom}), 7.85 d (2H, J = 8.0, 7.2 Hz, H_{arom}), 9.79 s (2H, NH_2). ^{13}C NMR spectrum, δ_C, ppm: 35.6 (CH_3), 103.6, 110.5, 112.8, 112.9, 116.2, 118.3, 120.2, 122.6, 124.6, 132.2, 136.2, 140.2, 142.8, 152.3, 157.2, 162.6, 172.2 (C=O). Mass spectrum: *m*/*z* 378.23.

CONCLUSIONS

The synthesis of novel $MgMnO_3$@ZrO_2@CoO core–shell catalyst by simple hydrothermal method has been reported for the first time. The catalyst was used for the one-pot three-component synthesis of dihydropyrano[3,2-*c*]chromene derivatives from 4-hydroxycoumarin, malononitrile, and substituted benzaldehydes. The salient features of this study include the use of easily available materials, higher yields, shorter reaction time, cleaner reaction conditions, and catalyst reusability. With reference to our study, this method is a useful alternative to many other complicated reactions reported so far.

ACKNOWLEDGMENTS

The authors thank S. P. Pune University (Pune, Maharashtra) for financial support, and SAIF Cochin (Kerala, India) for supporting analytical studies.

CONFLICT OF INTEREST

The authors declare no conflict of interest.

REFERENCES

1. Domlin g, A., *Chem. Rev*., 2006, vol. 106, p. 17. https://doi.org/10.1021/cr0505728
2. Ugi, I., *Adv. Synth. Catal*., 1997, vol. 339, p. 499. https://doi.org/10.1002/prac.19973390193
3. Terrett, N.K., Gardner, M., Gordon, D.W., Kobylecki, R.J., and Steele, J., *Tetrahedron*, 1995, vol. 51, p. 8135. https://doi.org/10.1016/0040-4020(95)00467-M
4. Dömling, A. and Ugi, I., *Angew. Chem., Int. Ed*., 2000, vol. 39, p. 3168. https://doi.org/10.1002/1521-3773(20000915)39:18<3168::AID-ANIE3168>3.0.CO;2-U
5. Kandhasamy, K. and Gnanasambandam, V., *Curr. Org. Chem*., 2009, vol. 13, p. 1820. https://doi.org/10.2174/138527209789630514
6. Bienaymé, H., Hulme, C., Oddon, G., and Schmitt, P., *Chem. Eur. J*., 2000, vol. 6, p. 3321. https://doi.org/10.1002/1521-3765(20000915)6:18<3321::AID-CHEM3321>3.0.CO;2-A
7. Müller, T.J.J., *Science of Synthesis, Multicomponent Reactions I*, Stuttgart: Georg Thieme, 2014, vol. 1. https://doi.org/10.1055/b-003-125816
8. Borhade, A.V., Tope, D.R., Gare, G.D., and Dabhade, G.B., *J. Korean Chem. Soc*., 2017, vol. 61, p. 157. https://doi.org/10.5012/jkcs.2017.61.4.157
9. Tope, D.R., Patil, D.R., and Borhade, A.V., *J. Chem. Pharm. Res*., 2012, vol. 4, p. 2501.
10. Borhade, A.V., Uphade, B.K., and Tope, D.R., *J. Chem. Sci*., 2013, vol. 125, p. 583. https://doi.org/10.1007/s12039-013-0396-8
11. Szabó, D.V. and Vollath, D., *Adv. Mater*., 1999, vol. 11, p. 1313. https://doi.org/10.1002/(SICI)1521-4095(199910)11:15<1313::AID-ADMA1313>3.0.CO;2-2
12. Dumitrache, F., *Diamond Relat. Mater*., 2004, vol. 13, p. 362. https://doi.org/10.1016/j.diamond.2003.10.022
13. Borhade, A.V., Tope, D.R., Agashe, J.A., and Kushare, S.S., *J. Water Environ. Nanotechnol*., 2021, vol. 6, p. 164. https://doi.org/10.22090/jwent.2021.02.006
14. Borhade, A.V., Tope, D.R., Agashe, J.A., and Kushare, S.S., *J. Water Environ. Nanotechnol*., 2021, vol. 6, p. 306. https://doi.org/10.22090/jwent.2021.538176.1427
15. Larios, E., Calderón, L., Guerrero, K., Pinedo, E., Maldonado, A., and Tanori, J., *J. Dispersion Sci. Technol*., 2012, vol. 33, p. 1360. https://doi.org/10.1080/01932690903294147

16. Green, G.R., Evans, J.M., and Vong, A.K., *Comprehensive Heterocyclic Chemistry II*, Katritzky, A.R., Rees, C.W., and Scriven, E.F.V., Eds., Oxford: Pergamon, 1996, vol. 5, p. 469. https://doi.org/10.1016/B978-008096518-5.00112-X
17. Foye, W.O. and Dall'Acqua, F., *Principi di chimica farmaceutica*, Padova: Piccin, 1991, 2nd ed., p. 416.
18. Konkoy, C.S., Fick, D.B., Cai, S.X., Lan, N.C., and Keana, J.F.W., US Patent no. 6800657B2, 2004.
19. Burgard, A., Lang, H., and Gerlach, U., *Tetrahedron*, 1999, vol. 55, p. 7555. https://doi.org/10.1016/S0040-4020(99)00376-2
20. Evans, J.M., Fake, C.S., Hamilton, T.C., Poyser, R.H., and Showell, G.A., *J. Med. Chem*., 1984, vol. 27, p. 1127. https://doi.org/10.1021/jm00375a007
21. Evans, J.M., Fake, C.S., Hamilton, T.C., Poyser, R.H., and Watts, E.A., *J. Med. Chem*., 1983, vol. 26, p. 1582. https://doi.org/10.1021/jm00365a007
22. Khaleghi-Abbasabadi, M. and Azarifar, D., *Res. Chem. Intermed*., 2019, vol. 45, p. 2095. https://doi.org/10.1007/s11164-018-03722-y
23. Mohammaadi, P. and Sheibani, H., *Mater. Chem. Phys*., 2019, vol. 228, p. 140. https://doi.org/10.1016/j.matchemphys.2018.11.058
24. Wanzheng, M.A., Ebadi, A.G., Sabil, M.S., Javahershenasd, R., and Jimenez, G., *RSC Adv*., 2019, vol. 9, p. 12801. https://doi.org/10.1039/c9ra01679a
25. Ramin, G.V., Jafar, M., Yaser, M., and Azadeh, S., *Curr. Org. Synth*., 2017, vol. 6, p. 904. https://doi.org/10.2174/1570179414666170203150629
26. Jain, S., Rajguru, D., Keshwal, B.S., and Acharya, A.D., *Int. Scholarly Res. Not*., 2013, vol. 2013, article ID 185120. https://doi.org/10.1155/2013/185120
27. Emtiazi, H. and Amrollahi, M.A., *Bulg. Chem. Commun*., 2017, vol. 49, p. 478.
28. Kanakaraju, S., Prasanna, B., Basavoju, S., and Chandramouli, G.V.P., *Arab. J. Chem*., 2017, vol. 10, p. S2705. https://doi.org/10.1016/j.arabjc.2013.10.014
29. Khurana, J.M., Nand, B., and Saluja, P., *Tetrahedron*, 2010, vol. 66, p. 5637. https://doi.org/10.1016/j.tet.2010.05.082
30. Abdolmohammadi, S. and Balalaie, S., *Tetrahedron Lett*., 2007, vol. 48, p. 3299. https://doi.org/10.1016/j.tetlet.2007.02.135
31. Shitole, B.V., Shitole, N.V., and Kakde, G.K., *Orbital: Electron. J. Chem*., 2019, vol. 9, p. 131. https://doi.org/10.17807/orbital.v11i3.1396
32. Kidwai, M. and Saxena, S., *Synth. Commun*., 2006, vol. 36, p. 2737. https://doi.org/10.1080/00397910600764774
33. Mohammadi, A.S., and Balalaie, S., *Tetrahedron Lett*., 2007, vol. 48, p. 3299. https://doi.org/10.1016/j.tetlet.2007.02.135
34. Khurana, J.M. and Kumar, S., *Tetrahedron Lett*., 2009, vol. 50, p. 4125. https://doi.org/10.1016/j.tetlet.2009.04.125
35. Shaabani, A., Samadi, S., Badri, Z., and Rahmati, A., *Catal. Lett*., 2005, vol. 104, p. 39. https://doi.org/10.1007/s10562-005-7433-2
36. Tavakoli-Hoseini, N., Heravi, M.M., Bamoharram, F.F., and Davoodnia, A., *Asian J. Chem*., 2011, vol. 23, p. 3599.
37. Dekamin, M.G., Eslami, M., and Maleki, A., *Tetrahedron*, 2013, vol. 69, p. 1074. https://doi.org/10.1016/j.tet.2012.11.068
38. Borhade, A.V., Tope, D.R., and Agashe, J.A., *J. Mater. Sci.: Mater. Electron*., 2018, vol. 29, p. 7551. https://doi.org/10.1007/s10854-018-8747-3
39. Heshmatpour, F. and Aghakhanpour, R.B., *Powder Technol*., 2011, vol. 205, p. 193. https://doi.org/10.1016/j.powtec.2010.09.011
40. Singh, A.K. and Nakate, U.T., *Sci. World J*., 2014, vol. 2014, article ID 349457. https://doi.org/10.1155/2014/349457
41. Pudukudy, M., Yaakob, Z., Narayanan, B., Gopalakrishnan, A., and Tasirin, S.M., *Superlattices Microstruct*., 2013, vol. 64, p. 15. https://doi.org/10.1016/j.spmi.2013.09.012
42. Yuan, Y., Ye, F., and Li, S., *Mater. Lett*., 2006, vol. 60, p. 3175. https://doi.org/10.1016/j.matlet.2006.02.062
43. Hekmatshoar, R., Majedi, S., and Bakhtiari, K., *Catal. Commun*., 2008, vol. 9, p. 307. https://doi.org/10.1016/j.catcom.2007.06.016
44. Safaei-Ghomi, J., Eshteghal, F., and Shahbazi-Alavi, H., *Polycyclic Aromat. Compd*., 2020, vol. 40, p. 13. https://doi.org/10.1080/10406638.2017.1348368
45. Zheng, J. and Li, Y.-Q., *Arch. Appl. Sci. Res*., 2011, vol. 3, no. 2, p. 381.
46. Pendalwar, S.S., Chakrawar, A.V., Chavan, A.S., and Bhusare, S.R., *Der. Pharma. Chem*., 2016, vol. 8, no. 10, p. 143.